

Hongxiang Gao, Zhenghua Chen and Min Wu are with Institute for Infocomm Research, A*STAR, Singapore 138632, Singapore (e-mails: {Chen.Zhenghua, wumin}@i2r.a-star.edu.sg).

Hongxiang Gao, Xingyao Wang, Zhenghua Chen, *Senior Member, IEEE*, Min Wu, *Senior Member, IEEE*, Jianqing Li and Chengyu Liu, *Senior Member, IEEE*

Index Terms—wearable, electrocardiogram interpretation, multi-resolution, continual learning

I. INTRODUCTION

CARDIOVASCULAR diseases (CVDs) are the leading cause of worldwide mortality and the largest contributor to a deterioration in life satisfaction [1]. Electrocardiogram (ECG) monitoring is currently a vital non-invasive method for cardiovascular risk event surveillance in order to detect relevant ischemia and malignant arrhythmia at an early stage. Despite advances in medical technology, the mortality rate from CVDs remains high. This is due to a variety of variables, including the lack of knowledge about CVDs among the general population, the transient nature of CVDs, and the absence of real-time diagnostic methods. Technically, the new wearable ECG monitoring equipment is long-term, continuous, noninvasive, and dynamic. It is also cost-effective, adaptable, and simple to set up, making it ideal for daily monitoring and early detection of CVDs [2], [3]. Having a real-time and reliable diagnostic analysis available at the edge device is crucial for this kind of technology to be adopted in the marketplace. Development of algorithms for automated ECG interpretation is thus the most crucial step.

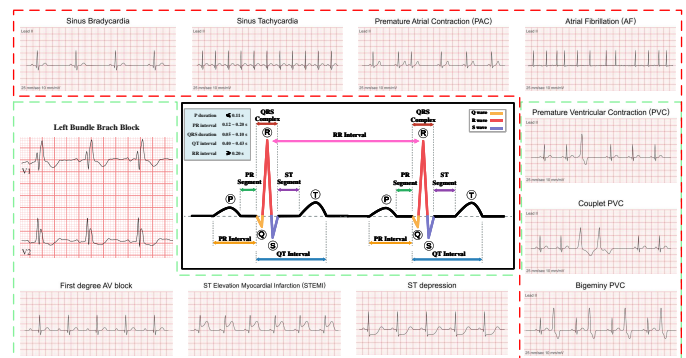


Fig. 1. Instances of common arrhythmias with aberrant ECG waveform shape (circled in red dashed box) and irregular rhythm (circled in green dashed box). The overlap region suggests that both qualities are abnormal. Extensive data on heartbeat morphology and rhythm intervals are included in the central example graphic.

Significant advancements have been achieved in ECG interpretation over the last several decades, and numerous new

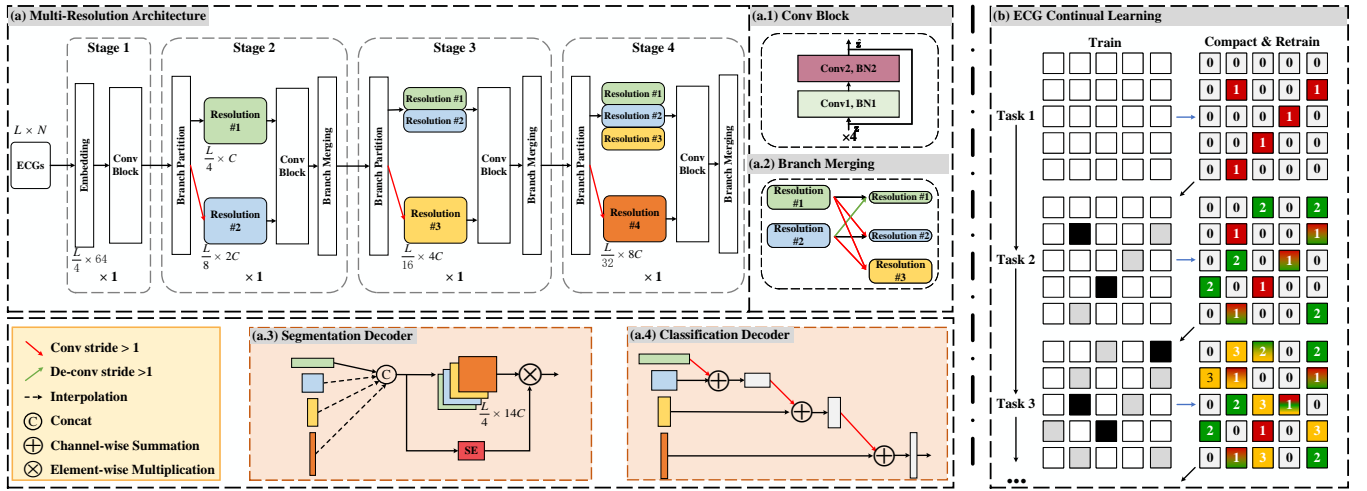


Fig. 2. (a) Multi-resolution architecture with the Conv block (a.1), the branch merging module (a.2), the segmentation decoder (a.3), and the classification decoder (a.4), and (b) an illustration of continuous learning on model parameters. The multi-resolution architecture is applicable to all tasks, while the two decoders are exclusively applicable to segmentation tasks or classification tasks respectively. All shared weights are subject to a continual learning approach. The following are some remarks concerning clause (b): Empty cells in the train matrix are available for training, whereas grey cells are utilized primarily for forward training and black cells are frozen. In the compact & retrain matrix, t -filled cells indicate the weights for Task t , zero indicates released parameters, and the gradient color indicates the weights are utilized for more than one task.

open-source resources, like as databases [4]–[7] and algorithms [8]–[12], have been published. The majority of ECG analysis involves segmenting significant waves, such as QRS complexes, P waves, and T waves, and classifying arrhythmias with aberrant morphology and rhythm. Researchers have previously developed the QRS segmentation method by analyzing the QRS complex’s morphological, rhythmic, and amplitude characteristics [9], [11]. The QRS morphological information and RR interval series are then utilized to develop classification algorithms for arrhythmias based on clinical background knowledge. With the development of deep learning algorithms, it is no longer essential to identify the QRS prior to categorizing ECG events. Deep learning-based approaches separate the segmentation and classification processes into distinct models and achieve the state-of-the-art performance on all tasks [13]–[19]. Nonetheless, the following three challenges to the widespread usage of wearable devices are outside the scope of these strategies: 1) insufficient utilization of low- and high-resolution information to integrate contextual and semantic knowledge for the final decision; 2) the difficulty in developing generalizable models stems from the fact that ECG datasets tend to be tiny and inconsistent in attribute type or data dimension; and 3) the morphology and rhythm of the QRS waveform, for example, are crucial for precise QRS location and greatly contribute to categorizing (as shown in Figure 1), but there is no efficient method for transmitting this learning.

In computer vision, the notion of learning at several resolutions has garnered considerable attention [20]–[22]. Typically, convolutional neural networks (CNNs) for image classification learn progressively from high to low resolution, followed by a final prediction. To accomplish reliable prediction, models such as FPN [23] and Unet [24] were developed to integrate high-resolution information (also known as local feature) from the beginning layers with low-resolution information (also known as global feature) from the deeper layers. ResNet, a

typical low-resolution decision model, was originally used by Wang *et al.* [8] for classification with less fundamental block settings. Later, with the availability of larger open-access physiological classification datasets [5], [6], [25] and challenging QRS segmentation datasets [4], [7], the usage of CNNs for feature extraction and recurrent neural networks (RNNs) for temporal dependency capture was explored within a deep learning paradigm [26]–[29]. However, these are just straightforward technique applications. ECGs feature a characteristic pseudo-periodicity and a rigid morphological distribution, both of which are the most essential clinical diagnostic criteria, and hence demand further consideration. Cai *et al.* [10] suggested three convolution branches with varying dilation rates to account for varying visual scales. Their solution won the 2019 China Physiological Signal Challenge (CPSC) with the highest score. To gather multi-resolution information, researchers expand the convolution kernel and the dilation window [8], [30]. However, these approaches yield distinct resolution characteristics separately and without interaction.

To this end, we proposed a CNN-based multi-resolution architecture that retains high resolution throughout the learning process (Figure 2 (a)). At each training phase, the high-resolution branch is maintained while a new low-resolution branch is added. By mutually integrating the trained branches from the previous step, it is possible to keep both local and global characteristics in all branches. The convolution module is meticulously designed such that the high-resolution branch can discern a QRS duration width filed while the low-resolution branch can detect two consecutive QRS intervals. We also constructed heuristically a segmentation decoder (Figure 2(a.3)) based on multi-resolution and a classification decoder (Figure 2(a.4)) based on low-resolution.

In terms of data, the PhysioNet/Computing in Cardiology Challenge (CinC) 2020 [31] is by far the largest collection

of open-access ECG recordings from six medical centers. However, each dataset has a distinctive cardiac abnormality, and the class is distributed in a long-tail pattern, making it more difficult to develop a robust model. Currently, researchers use all available datasets and train the final classifier utilizing the whole number of categories. Clearly, such an approach would worsen the model's performance by increasing the imbalance of categorical distribution.

Multiple comparable works exist for the third challenge. Salem *et al.* [32] advocated transferring model information from computer vision tasks, which we now refer to as finetune. Kuba *et al.* [33] pretrained a model on huge ECG datasets and then optimized it for specific classification tasks. Raza *et al.* [34] used federal knowledge to denoise ECG before transferring the information for categorization. All of these approaches, however, focus on small datasets and use transfer learning in fine-tune mode. Kiyasseh *et al.* [35] proposed an ECG approach for continuous learning from the perspective of acquired data source, individual variation, and categorization increase. To our knowledge, no efforts have been made to overcome the problem of transferring information from segmentation to classification.

As seen in Figure 2 (b), we solve the aforementioned two challenges utilizing a parameter isolation-based continual learning approach. Specifically, we address the data deficiency and label inconsistency issues by integrating valuable information from each dataset using class-incremental continual learning. We address the issue of knowledge transfer by sequentially learning single-, multi-lead segmentation, minority-, and multiple-class categorization problems using a domain-incremental continual learning approach. The process sharing generic features from previous tasks and generate specific features on current task. Moreover meaningful, QRS complex segmentation is likely to make use of the QRS duration, QRS morphology, RR interval, and other baseline information, all of which are essential diagnostic references in clinical situations. We believe this will benefit future endeavors. Extensive experiments have proven our hypothesis. In addition, it is more clinically acceptable to forecast the given recording's super-class, such as sinus, atrial, or ventricular aberrant, and then categorize it more precisely according to its particular abnormalities. Our approach of continuous learning might accomplish segmentation and hierarchical classification without requiring additional model storage space.

The main contributions of this paper are summarized as follows:

- 1) We propose a novel CNN-based multi-resolution model for preserving both high-resolution morphological semantic and low-level rhythmical features. With a well-designed convolution module, our models are capable of both classification and segmentation.
- 2) We are the first to propose merging segmentation and classification tasks in a unified framework, employing generic features to boost performance on downstream tasks and training task-specific features to solve the present problem, which are also acceptable in solving data limits for a more comprehensive ECG interpreter.
- 3) We conduct extensive experiments by grouping ECG

interpretation tasks on CPSC 2019 [4], 12-lead QRS [7], ICBEB 2018 [5] and PTBXL [25], four publicly available datasets. The experimental results demonstrate our ECG-CL approach are able to interpret ECG in a more comprehensive way and results on sing-lead experiment prove our prospective application for wearable devices.

II. RELATED WORKS

A. Deep Learning-Based ECG Analysis

The collected information from individual ECGs is intrinsically multi-level, consisting of semantic segmentation [36], [37] and rhythm and morphological anomaly detection [14]–[17], [38]. With the advent of wearable ECG monitoring, rule-based approaches are no longer applicable to dynamically complicated situations ECG analysis has progressively been dominated by deep learning based techniques. The majority of the research focused on end-to-end processes, such as anomaly classification [18]. CNNs, RNNs, and CNN+RNN are the most frequent architectures used to describe spatial attention and temporal dependence. ECG displays a time series with a single or multiple channels; hence, the spatial characteristics of a single-lead ECG may be interpreted as local temporal characteristics. The capacity of a well-designed CNN to extract inter-channel characteristics enables it to outperform RNNs in multi-lead ECG modeling while achieving similar performance in single-lead ECG modeling. ECG segmentation is practically performed on a single lead [10], while classification typically requires information from many channels. Researchers using deep learning do segmentation and classification separately. In addition, a number of studies combined heartbeat segmentation to get more exact and interpretable results [19], [39], [40]. However, their solution utilizes heartbeat data provided by the dataset or calculated using existing QRS localization algorithms. Such approaches consider each step of ECG analysis to be independent and distribute a different deep learning model for each stage; nevertheless, they are not application efficient. In this research, we use continual learning to handle multi-level ECG analysis inside a single framework, therefore greatly improving efficiency.

B. Multi-resolution Neural Networks

Multi-resolution merging is widely researched in [20]–[22]. The straightforward way is to feed multi resolution inputs paralleled into multiple networks and aggregate the output response maps [10]. U-Net [24] combine low-level features in the downsample process into the same resolution high-level features in the upsample process progressively through skip connections. Pyramid based models fuse the hierarchical features from feature pooling procedure. HRNet [21] recommended maintaining high-resolution elements throughout the training operation. All of these approaches are intended for images that depict as a square matrix. ECGs are often recorded with a high sample frequency, which makes it difficult to maintain high-resolution data, i.e. characteristics in limited network reception fields. Local morphological information and global rhythm information are essential no matter the segmentation and classification tasks for ECG. In this document,

we suggested a CNN-based multi-resolution network as the encoder and segmentation and classification-specific decoder.

C. Continual Learning

Continual learning is a kind of multi-task machine learning approach designed to promote algorithms to progress in a manner analogous to human learning via the transfer of acquired information and the prevention of forgetting. According to Van de Cen and Tolia [41], continual learning may be categorized into three distinct scenarios: (i) task-incremental learning, (ii) domain-incremental learning, and (iii) class-incremental learning. Computer vision tasks have used continual learning approaches for a considerable length of time. In general, these strategies may be categorized into three broad groups: memory-based, regulation-based, and parameter isolation-based [42]. Parameters and hyperparameters of a model are often constrained using regularization-based approaches [43]–[46]. This is done so that the model can recall previously learnt information while learning new tasks. Memory-based techniques [47]–[49] often contain a memory buffer to hold data instances and/or other information connected to prior activities. This knowledge is then played back during the learning of new tasks to reinforce what has been previously learnt and avoid "catastrophic forgetting." Typically, parameter isolation-based approaches [50]–[52] provide distinctive model parameters to consecutive jobs so that upcoming tasks do not conflict with what was previously learnt.

ECG interpretation is comprised mostly of segmentation for heart rate-related calculations and segment classification for abnormal diagnosis. Deep learning-based QRS segmentation is seen as a time-point binary classification, and continual learning over several datasets is more closer to a class-incremental task in which new unseen QRS morphology must be identified. The limitations of the dataset include its limited size, inaccurate labelling, and anomalous class distribution. Continual learning inside classification tasks is a class-incremental scenario that may incorporate all non-unified classification datasets into a comprehensive general abnormal classification model. In addition, segmentation characteristics are definitely beneficial for classification tasks, as stated by the clinical diagnostic standard and shown in Figure 1. Continual learning from segmentation to classification could be viewed as a domain-incremental scenario. We solve all these three continual learning issue in this paper based on the parameter isolation technique.

III. METHODS

A. Task Definition

The goal of electrocardiogram (ECG) segmentation is to pinpoint the most apparent waves, often QRS complexes (reflecting heartbeat), whereas the objective of ECG classification is to identify the kind of arrhythmia based on an acquired ECG recording. Algorithmically, wearable devices place heavy emphasis on the capacity for segmentation and classification. We presented an universal multi-resolution architecture for ECG signal interpretation based on its inherent characteristics. Existing datasets are tiny and inconsistent in labeling, and

existing models are deployed in a sequential sequence, which is wasteful for storage and processing. We want to construct domain-incremental continual learning to integrate segmentation and classification, and class-incremental continual learning to address the inconsistent dataset problem. Suppose we independently perform ECG segmentation and classification on several datasets using the same model. The objective of ECG continual learning is to apply the information obtained from previous tasks to learn a more accurate representation and classifier for the next challenge, while avoiding forgetting.

B. Convolution-Based High-Resolution Modeling for ECGs

1) *Multi-resolution Encoder*: An overview of the the Multi-Resolution architecture is presented in Figure 2 (a), which illustrates the tiny version. Consider an ECG input $\mathbf{X} \in \mathbb{R}^{L \times N}$ with L denotes the signal length and N is the number of leads. A convolutional embedding layer is applied on this raw-valued signal to project it to an arbitrary channel dimension (64 adopted in this paper) and reduce the size along the length dimension to a quarter. It is worthy noting that in order to construct an unified framework for different ECG clips, we add a 1×1 convolution layer to project the ECGs collected from non-standard devices to 12 channels. Several basic residual blocks (Conv blocks, as shown in Figure 2 (a.1)) are applied on these embedding. The Conv blocks Figure 2 (a.1) maintain the resolution of signals ($1 \times \frac{L}{4}$), and together with the embedding module are referred to as "Stage 1".

In order to produce hierarchical representation, the size of each channel is reduced by branch partition layers as the network gets deeper. The first branch partition layer maintain the initial embedded feature shape, and applies a stride convolution to obtain more high-level embedding. This decrease the number of features in each channel to a half ($2 \times$ down-sampling of resolution, i.e., $1 \times \frac{L}{8}$), and the output dimension is set to $2C$. Conv Blocks are applied afterwards for feature transformation, with the resolution as the shape of input branch. A branch merging layer (as shown in Figure 2 (a.2)) is applied afterwards to generate local-global effective semantics. This first block of branch branch partition, feature transformation and branch merging is denoted as "Stage 2". The procedure is repeated twice, as "Stage 3" and "Stage 4", with the lowest resolutions of $1 \times \frac{L}{16}$ and $1 \times \frac{L}{32}$, respectively. These stages jointly produce a hierarchical representation for high-level semantic while maintain the high-resolution semantic at the same time. As a result, the propose architecture are suitable ECG interpretation.

2) *Segmentation Decoder*: As we suppose to deal with both ECG segmentation and classification tasks, segmentation decoder and classification decoder are proposed following the main backbone. ECG segmentation, somehow like a object detection task in time series, deserved more high-resolution information for final decision. We interpolate the lower-resolution representations to the same shape as the highest resolution representation, and apply a SE module for more concrete attention on effective semantics, as shown in Figure

2 (a.3). The segmentation decoder can be represented as:

$$\mathbf{Z} = \text{Concat}(\mathbf{z}_0, \mathcal{I}(\mathbf{z}_1), \mathcal{I}(\mathbf{z}_2), \mathcal{I}(\mathbf{z}_3)) \quad (1)$$

$$\hat{\mathbf{Z}} = \mathbf{Z} \odot \text{SE}(\mathbf{Z}), \quad (2)$$

$$\mathbf{O}_{\text{seg}} = \text{Sigmoid}(w \cdot (\text{AAP}(\hat{\mathbf{Z}})) + b), \quad (3)$$

where $\mathbf{z}_0 \in \mathbb{R}^{C \times \frac{L}{4}}$, $\mathbf{z}_1 \in \mathbb{R}^{2C \times \frac{L}{8}}$, $\mathbf{z}_3 \in \mathbb{R}^{4C \times \frac{L}{16}}$, and $\mathbf{z}_4 \in \mathbb{R}^{8C \times \frac{L}{32}}$, $\mathbf{Z} \in \mathbb{R}^{14C \times \frac{L}{4}}$, $\mathcal{I}(\cdot)$ denotes the interpolation function, SE denotes the Squeeze-and-Excitation module [53], \odot denotes the element-wise multiplication, w and b are the parameter of fully connected layer and AAP(\cdot) denotes the Adaptive Average Pooling function. Finally, the output logits $\mathbf{O}_{\text{seg}} \in \mathbb{R}^{\frac{L}{4}}$ with value greater than 0.5 denotes the possible point-of-interest.

3) *Classification Decoder*: Similarly, we design the classification decoder based on the multi-resolution output and transpose them to a low-dimension representation for categorical decision, as shown in Figure 2 (a.4). Instead of using the lowest resolution representation directly as traditional classification models done, we gradually introduce the high-resolution representation into the lower resolution by strided convolution and channel-wise summation. The classification decoder can be represented as:

$$\hat{\mathbf{z}}_{i+1} = \mathbf{SConv}(\mathbf{z}_i) \oplus \mathbf{z}_{i+1}, \quad s.t. \quad i \in \{0, 1, 2\}, \quad (4)$$

$$\mathbf{Z} = \hat{\mathbf{z}}_3, \quad (5)$$

$$\mathbf{O}_{\text{cls}} = \text{Sigmoid}(w \cdot \text{GAP}(\mathbf{Z})) + b, \quad (6)$$

where \mathbf{SConv} denotes the strided convolution, \oplus denotes the channel-wise summation, $\text{GAP}(\cdot)$ denotes the global average pooling layer, w and b denotes the parameter of fully connected layer. $\mathbf{O}_{\text{cls}} \in \mathbb{R}^n$ denotes the n -class multi-label logits.

C. ECG Continual Learning

1) *Motivation*: To generate a unified model with the ability of: 1) realizing segmentation and classification in an efficient storage burden and computation overload, 2) dealing with increasing data and unseen class in the future in a lifelong learning mode, and 3) without forgetting of the previous learned tasks. A possible way is to preserve the old-task weights that are already optimized and expand the network structure by adding depth and width when training new tasks. It is intuitive that there exist generic concepts that characterize reviews across different domains (as shown in Figure 1), which is favorable for knowledge transfer across domains. In most previous architecture-based continual learning methods, the whole framework for old tasks are frozen to avoid forgetting, and the weights are used for feature sharing to new tasks. However, the storage or memory complexity of the model is in a fold increase with the quantity of tasks. Previous literature had proved the parameter redundancy of the CNNs for the current task. Since the use of all preserved weights, the fine-tuning for new task will be with partial of the domain generic knowledge while hard to generate domain specific knowledge. To tackle the above mentioned issues, we propose a iterative pruning with generic weights picking method.

In particular, this work follows a parameter-isolated continual learning scenario [52]. The backbone model and domain specific decoder has performed learning on a sequence of ECG interpretation tasks. We employ an iterative, three-stage framework for a unified ECG interpretation. The multi-resolution architecture is a general backbone network used for feature encoder and thus is shareable to both segmentation tasks and classification tasks. The proposed decoders are exclusive between dissimilar tasks while shareable within similar tasks. The continual learning technique is conducted on these shareable weights by iterative train-compact-retrain on every task. Considering the complexity of general ECG interpretation as data incremental for segmentation task, class-incremental for classification task, and domain incremental for transfer from segmentation to classification tasks.

2) *Continual Training*: Let \mathcal{T} be the total set of tasks, \mathcal{T}^S and \mathcal{T}^C denotes the set of segmentation and classification tasks, i.e., $\mathcal{T} = \mathcal{T}^S \cup \mathcal{T}^C$. Let t, s, c denotes the index of the current task in total tasks and in segmentation or classification tasks, then $t = s + c$.

Task \mathcal{T}_1 : As shown in the first row in Figure 2 (b), we train an initial network from scratch for the first task \mathcal{T}_1 and then prune the weights to a preset sparsity. Afterwards, another short fine-tuning step with little learning rate is applied to recover the performance caused by violent weights pruning. Let the preserved encoder weights for the first task as $W_{\text{MR}_1}^P$ and the released weights as $W_{\text{MR}_1}^R$. The same procedure is conducted to the two decoders, and the preserved weights and released weights for the first segmentation task is $W_{\text{Seg}_1}^R, W_{\text{Seg}_1}^P$ and $W_{\text{Cls}_1}^R, W_{\text{Cls}_1}^P$ for the first classification task, respectively.

Task $\mathcal{T}_t \rightarrow \mathcal{T}_{t+1}$: Suppose we have completed the learning on tasks $\mathcal{T}_{1:t}$ containing s segmentation tasks and c classification tasks. We denotes the model weights preserved for segmentation tasks $\mathcal{T}_{1:s}^S$ as $W_s^P = W_{\text{MR}_{1:t}}^P \cup W_{\text{Seg}_{1:s}}^P$ and model weights preserved for classification tasks $\mathcal{T}_{1:c}^C$ as $W_c^P = W_{\text{MR}_{1:t}}^P \cup W_{\text{Cls}_{1:c}}^P$. We trained weights picking masks M_s and M_c on the preserved weights to select generic features from previous tasks to transfer favorable knowledge to downstream tasks. When dealing with a new task \mathcal{T}_{t+1} , for example, we assume it belongs to a classification task here. We first train a network with the mask-picked weights $W_c^P \odot M_c$, which are used to provide the generic knowledge and the released weights $W_c^R = W_{\text{MR}_t}^R \cup W_{\text{Cls}_c}^R$ which are used to replenish task \mathcal{T}_{t+1} specific weights. Noted that, the gradient of the picked weights are set as zero to maintain the performance on past task. Afterwards, prune and retrain step was added to make room for next task and recover performance on current task. We repeat the above described three-stage pattern until all tasks have been learned.

3) *Inference*: When performing inference for a given task, the task ID should be confirmed first to acquire the task-related parameters leveraging the preserved binary masks. As we all known, model weight loading occupies most of the inference time especially for cascaded multi-task inference. However, our continual learning technique trained model only need to be loaded once at the beginning, even if facing the sequential multi-task scenario. The sequential inference realized by leveraging the task-ID filled binary masks.

Algorithm 1 Comprehensive ECG continual learning strategy.

Input: Pretrained encoder for task \mathcal{T}_1 ; segmentation decoder for task \mathcal{T}_1^S ; classification decoder for task \mathcal{T}_1^C ; training mode m (*Seg* or *Cls*).

Output: The ECG interpreter for tasks \mathcal{T}_1 to \mathcal{T}_T .

```

1: while  $t = 1$  do
2:   if  $m_1 == \text{Seg}$  then
3:     Perform prune and retrain. Let the preserved weights
       be  $W_1^P = W_{MR_1}^P \cup W_{Seg_1}^P$  and the released weights
       be  $W_1^R = W_{MR_1}^R \cup W_{Seg_1}^R$ ;
4:   else if  $m_1 == \text{Cls}$  then
5:     Perform prune and retrain. Let the preserved weights
       be  $W_1^P = W_{MR_1}^P \cup W_{Cls_1}^P$  and the released weights be
        $W_1^R = W_{MR_1}^R \cup W_{Cls_1}^R$ ;
6:   end if
7: end while
8: if  $t \leq T$  then
9:   Assert  $s$  segmentation tasks  $c$  classifications tasks included, i.e.,  $t = s + c$ ;
10:  if  $m_t == \text{Seg}$  then
11:    Preserved weights  $W_{t-1}^P = W_{MR_{1:t-1}}^P \cup W_{Seg_{1:s-1}}^P$ ;
12:    Released weights  $W_{t-1}^R = W_{MR_{1:t-1}}^R \cup W_{Seg_{1:s-1}}^R$ .
13:  else if  $m_t == \text{Cls}$  then
14:    Preserved weights  $W_{t-1}^P = W_{MR_{1:t-1}}^P \cup W_{Cls_{1:c-1}}^P$ ;
15:    Released weights  $W_{t-1}^R = W_{MR_{1:t-1}}^R \cup W_{Cls_{1:c-1}}^R$ .
16:  end if
17:  Train task  $\mathcal{T}_t$  using mask-picked weights and released weights:  $(M_{t-1} \odot W_{t-1}^P) \cup W_{t-1}^R$ ;
18:  Perform prune and retrain, update the preserved weights  $W_t^P$  and released weights  $W_t^R$  and the mask  $M_t$ ;
19:   $t = t + 1$ .
20: end if

```

Using in real-life ECG interpretation, assume we have trained a four tasks continual learning model, e.g., *single lead segmentation* \rightarrow *multi-lead-segmentation* \rightarrow *limited-class classification* \rightarrow *multi-class classification*. An automatic ECG interpretation containing ECG segmentation and classification can be realized adaptively according to the input data shape. Given an input ECG episode, we select the lead related segmentation model and classify it using the most comprehensive classification model by default. Moreover, we can manually define the task ID sequence according to the real demands.

The network train-prune-retrain procedures are performed iteratively for learning multiple new tasks. We summarize the overall learning process of ECG continual learning in Algorithm 1.

IV. EXPERIMENTAL SETTINGS AND RESULTS

In this section, we first briefly introduce four datasets used in our experiments and the implementation details. We then perform five kinds of continual learning scheme to verify the effectiveness of proposed method.

TABLE I
DATASET DESCRIPTION

Dataset	Annotation	Sampling rate	Length	#Leads	#recordings
CPSC 2019	QRS	500	10 s	1	2000
12-lead QRS	QRS	500	10 s	12	9364
ICBEB 2018	9 classes	500	6-60 s	12	6877
PTBXL	71 classes	500	10 s	12	21873

A. Datasets

We test our method using two QRS segmentation datasets and two classification datasets, namely CPSC2019 [4] and 12-lead QRS [7], ICBEB 2018 [5] and PTBXL [25], summarized in Table I.

CPSC 2019 was released during the 2-nd CPSC in 2019 aiming to promote the QRS detection development among wearable dynamic ECGs. 2000 challenging single-lead ECGs were manually well-selected with QRS-like artifacts, impulse, strong noise, extremely abnormal morphology and pathological abnormality. Each recording was pre-processed to 10-second length with sampling rate as 500 Hz. Three cardiologists were involved to annotate the QRS locations beat-by-beat and make sure the selected ECG clips are recognizable to trained humans.

12-lead QRS was the QRS annotated version of the 1-st CPSC in 2018. By truncating the 12-lead ECG using a 10-second window without overlap, 12-lead QRS contains 9364 beat-by-beat annotated ECGs. The sampling rate is 500 Hz. The QRS position is mainly provided based on the Lead-II or Lead-V5, which two are acknowledged with the most remarkable QRS complex.

ICBEB 2018 was rearranged on the basis of the 1-st CPSC in 2018, containing a total of 6877 annotated 12-lead ECGs from six hospital and eight arrhythmia types. Noted that, 918 recordings in the whole are annotated as "Normal", which means sinus ECG in this situation, i.e., sinus tachycardia and sinus bradycardia are all regarded as normal. Each recording lasts between 6 and 60 seconds and is annotated by up to three statements by up to three cardiologist.

PTBXL is by far the largest public ECG classification database with 21873 clinical 12-lead ECG records of 10 seconds length from 18885 patients. According the the SCP-ECG standard [54], 71 different statements decompose into 44 diagnostic, 12 rhythm and 19 morphological statements. Moreover, five super-classes and 24 sub-classes is provided for diagnostic. Each recording may have multiple statements.

B. Experimental Settings

1) **Data preprocessing:** We immediately retrieve the 10-second ECG recordings or generate them using non-overlapping sliding windows to use in segmentation and classification training. As primary ECGs are effective in certain frequency bands, we do data pre-processing to convert raw ECG signals to the desired frequency domain (0.5 - 45 Hz). In addition, we normalize the 10-second signal such that the mean is zero and the variance is one. We do not include any more data augmentation strategies into this work to keep the implementation as simple as possible.

TABLE II

HYPERPARAMETERS USED FOR MODEL TRAINING. OPTIM IS ABBREVIATION OF OPTIMIZER, LR IS ABBREVIATION OF LEARNING RATE, AND WD IS ABBREVIATION OF WEIGHT DECAY.

Dataset	Batch size	Optim	LR	WD	Epochs
CPSC 2019	64	Adam	0.001	1e-3	50
12-lead QRS	128	SGD	0.007	1e-3	50
ICBEB 2018	128	SGD	0.015	1e-3	50
PTBXL	128	SGD	0.500	1e-8	200

2) *Data splits*: We randomly split the segmentation dataset into train, validation and test sets by 70/20/10 for model training and hyperparameter tuning, respectively. Data splitting for classification dataset is same as the prior studies [30], which have been given in CinC 2020 [6] for a comparable experiment.

3) *Baselines*: To compare our multi-resolution architecture and ECG-CL to traditional CNNs-based ECG interpretation algorithms, we include the most effective baseline reported in previous literature: ResNet1d-wang [8], a previous classic CNN for time series. We compare the results of two modes for both network: training from scratch, continual learning. All modes are trained and evaluated on the same pre-processed data.

4) *Implementation details*: Training for all models was accomplished in Pytorch on two NVIDIA Tesla A100 GPUs. We use a tiny multi-resolution architecture containing 4 stages (four types of resolution) with each stage contains 4 Conv Blocks. Model parameters for training from scratch and the first task in continual learning mode were randomly initialized. The threshold for both segmentation and classification logits are set as 0.5. We use a learning rate *warm-up* strategy for 5 epochs with an initial learning rate of 1e-6. The learning rate decays to a half every 30 epochs. For model pruning, the learning rate is set to a fixed value of 0.0005, the pruning ratio is set according to the number of tasks. Detailed hyperparameter settings are available in Table II.

5) *Evaluation metrics*: To realise comparable results with previous works, we adopt *F1*-score to assess the segmentation performance. We report the macro-averaged area under the receiver operating characteristic curve (henceforth referred to as AUC), which is obtained by averaging class-wise AUCs over all classes to assess the multi-label classification performance [25].

C. Experimental Results and Analysis

We conduct four kinds of continual learning experiments by grouping scenarios from the given datasets considering the possible application in real-life. In all experiments, model performance for each task is evaluated after all tasks have been learnt. ResNet_wang [8] shown excellent performance on ECG abnormal classification tasks [25] while efficient in model parameter at the same time is thus adopted here as a alternative backbone network. Continual learning have two prominent advantages: avoid catastrophic forgetting and forward knowledge transfer. To verify the first advantage, We conduct a "finetune" experiment by sequentially finetuning last well trained model on current dataset and report the results on

TABLE III

OVERALL DISCRIMINATIVE PERFORMANCE OF ECG CONTINUAL LEARNING ALGORITHMS ON SEQUENTIAL TASKS: *single-lead segmentation* → *multi-lead segmentation* → *fewer class classification* → *multiple class classification* IN TERMS OF F1_SCORE FOR SEGMENTATION TASKS AND MACRO AUC FOR CLASSIFICATION TASKS. FOR EACH TASK THE BEST-PERFORMING VALUE IS MARKED IN BOLD FACE. CL IS ABBREVIATION OF CONTINUAL LEARNING.

Model	Mode	CPSC 2019	12-lead QRS	ICBEB 2018	PTBXL
ResNet_wang	Scratch	98.83	99.93	96.90	91.90
	Finetune	91.24	97.39	92.30	92.11
	CL	98.87	99.98	96.93	92.56
ECG-CL	Scratch	99.04	99.91	97.30	92.18
	Finetune	91.22	96.99	92.87	92.35
	CL	99.12	99.98	98.03	92.73

each task using the final model weights. Noted that, we only finetune the shareable parameters like continual learning. To test forward knowledge transfer ability, we conduct "scratch" experiment by training each task a independent model from scratch, and evaluate the performance independently.

1) *Comprehensive cross-domain continual learning*: We first conduct the most comprehensive ECG interpretation method by continual learning on a sequential of four tasks. On the guidance of training model from low-level task to high level task and from simple task to complicate task, the task order and corresponding dataset is arranged as follows:

1. *single-lead segmentation*: CPSC 2019;
2. *multi-lead segmentation*: 12-lead QRS;
3. *fewer class classification*: ICBEB 2018;
4. *multiple class classification*: PTBXL-all.

The above experimental dataset arrives the model sequentially as the preset order. In this setting, each downstream task will produce task-specific features while benefit from the generic features from previous tasks. Consequently, the performance is supposed to surpass the model training from scratch. We can see that the accuracy on CPSC 2019 after prune is slight higher than train from scratch, this may due to the pruning have the weight regularization ability. Table III demonstrate the experimental results of our ECG-CL method and multi-resolution architecture. From the results, we can observe that the continual learning method outperforms training from scratch in downstream tasks. This is a strong support for our model are able to transfer generic information from previous tasks. More notably, the storage pressure of training multiple models from scratch is several times greater than that of continual learning model. Finetuning on new tasks exhibit comparable results on the last two classification tasks, but fail to preserve distinctive knowledge for the first two tasks and thus suffer a catastrophic forgetting.

2) *Continual learning classification from empirical perspective*: In clinical, ECGs are commonly interpreted by the P-QRS-T morphology and RR interval series. In PTBXL, all 71 classes are assigned to three non-mutually exclusive categories diagnosis (short for diagnostic statements such as "anterior myocardial infarction"), morphological (related to notable changes of particular segments within the ECG such as "abnormal QRS complex") and rhythmic (related to particular changes of the rhythm such as "atrial fibrillation"). Limiting

TABLE IV

CLASSIFICATION PERFORMANCE OF THE CONTINUAL LEARNING MODEL ON THREE DESCRIPTIVE ANOMALY TASKS ON PTBXL IN TERMS OF MACRO AUC.

Model	Mode	PTBXL-form	PTBXL-rythm	PTBXL-diag
ResNet_wang	Scratch	87.58	94.60	93.60
	CL	88.00	95.97	94.27
ECG-CL	Scratch	87.59	96.29	92.29
	CL	88.36	96.29	93.13

TABLE V

CLASSIFICATION PERFORMANCE OF THE CONTINUAL LEARNING MODEL ON FIVE DIAGNOSTIC TASKS ON PTBXL IN TERMS OF MACRO AUC.

Model	Mode	NORM	STTC	HYP	CD	MI
ResNet_wang	Scratch	94.97	91.53	90.48	92.73	93.58
	CL	95.20	86.70	92.63	93.33	93.40
ECG-CL	Scratch	96.25	88.25	94.44	94.12	93.67
	CL	96.77	90.18	95.55	95.99	93.81

TABLE VI

PERFORMANCE OF THE COMPREHENSIVE ECG CONTINUAL LEARNING MODEL FOR APPLICATION OF WEARABLE SMART DEVICES ON FOUR SINGLE-LEAD DATASETS IN TERMS OF F1_SCORE FOR SEGMENTATION TASK AND MACRO AUC FOR CLASSIFICATION TASK.

Model	Mode	CPSC 2019	rhythm	QRS form	ST-T form
ResNet_wang	Scratch	98.83	99.77	98.23	99.65
	CL	98.87	99.70	98.66	99.80
ECG-CL	Scratch	99.04	99.72	98.36	99.69
	CL	99.12	99.81	98.75	99.76

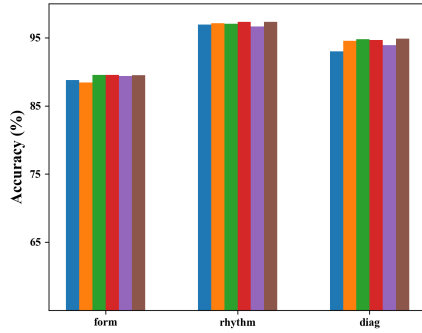


Fig. 3. Experimental results of ECG-CL with six learning order. Blue denotes the baseline result shown in Table.

the task to the classification of ECG abnormalities, PTBXL is currently the largest database of abnormalities and it is reasonable to assume that any existing ECG abnormalities not listed or to be identified in the future could be classified in the three categories above. Therefore, we trained the continuous learning model on the norm, rhythm, and diag types of the PTBXL database. Below is a description of the three types of tasks and the corresponding datasets.

1. 12-lead rhythm: PTBXL-form;
2. 12-lead form: PTBXL-rhythm;
3. 12-lead diagnosis: PTBXL-diag.

As there is no clear hierarchical relationship between these three tasks, we give the performance results in Table III for the above sequence. In addition, we explore the performance differences of six different curriculum learning in Figure 3.

From the figure we can see that the task order can slightly affect the whole performance, this may due to the similar classifying tasks.

3) Class-incremental learning from exclusive categories:

Multi-lead ECG signals used in clinical applications need to ultimately lead to reliable diagnoses that can assist physicians in improving efficiency or change the way multi-lead wearables such as the Holter are used. PTBXL contained 44 class of diagnosis commonly derived from clinical, and separate to five classes. However, there still are many diagnosis information not included, such as the malignant ventricular fibrillation, electrical axis offset, and etc. We design a task-incremental continual learning scheme with respect to cover all future possible new superclass or subclass. The five superclass provided in PTBXL is directly used in here to verify the model continual learning ability. In general, ST-T changes are a waveform phenomenon that can be associated with conduction block, myocardial infarction and hypertrophy. Pathological ST-T changes are not associated with other types. Myocardial infarction may be a trigger for conduction block and hypertrophy. Hypertrophy may contribute some conduction disturbance abnormal. We therefore set the sequential order as follows:

1. *super-class normal (NORM)*: PTBXL-NORM;
2. *super-class ST-T change (STTC)*: PTBXL-STTC;
3. *super-class hypertrophy (HYP)*: PTBXL-HYP;
4. *super-class conduction disturbance (CD)*: PTBXL-CD;
5. *super-class myocardial infarction (MI)*: PTBXL-MI.

For each super class, we take the basic statement for training samples rather than sub-class. Table V shows the comparison of two architectures in terms three training mode. The overall trend is consistent as former experiments while the continual learning results hold a large margin than training from scratch. This is because many basic cardiac abnormal usually arise accompanied with other pathological change.

4) *Continual learning for wearable application*: Wearable devices, such as smart watch (Apple Watch, Huawei Watch, Oppo Watch, Samsung, Fitbit) and portable ECG Monitor (AliveCor KardiaMobile ECG, Eko Duo) all adapt the upper

limb lead for its prominent exhibition in QRS amplitude. These devices are designed to help people keep closer tabs on their heart health, and can even be used to help identify atrial fibrillation a serious medical condition that is a leading cause of stroke. However, other kinds of cardiac abnormal are not yet developed to use in real-life environment. Single-lead ECG are able to diagnosis most common arrhythmias, such as premature atrial contraction (PAC), premature ventricular contraction (PVC), atrial fibrillation (AF) and other ST-T changed abnormal. We conduct the continual learning from single-lead segmentation to rhythmic, morphological classification to develop a robust wearable application pattern. Rhythmic classification based on heartbeat segmentation knowledge is easier than morphological classification, containing both aberrant QRS complexes and ST-T abnormal. We take the PAC, PVC and AF from ICBE2018 as the rhythmic abnormal dataset and PVC, right bundle branch block (RBBB), left bundle branch block (LBBB) as the QRS morphological abnormal dataset, and ST elevation STE and ST depression as the ST-T change dataset. It should be noted that we adopt signals from lead-I (collected as the suface electric potential difference from left hand to right hand) which are commonly used in wearable devices. In addition, bundle branch block exhibits obvious abnormal on lead-I. The sequential order is as follows:

1. *1-lead segmentation*: CPSC 2019;
2. *1-lead rhythm classification*: ICBE2018-rhythm;
3. *1-lead QRS form classification*: ICBE2018-form;
4. *1-lead ST-T form classification*: ICBE2018-STTC.

Table VI shows the comprehensive continual learning on single lead for wearable device prospective application. Results demonstrate compacting a sequential tasks within an model is feasible in wearable devices.

V. CONCLUSION AND FUTURE WORK

In this research, we present a multi-resolution architecture as the foundation of ECG interpretation tasks and a strategy for parameter-isolation-based continual learning. On this basis, we devised four types of continual learning experiments including domain incremental learning from segmentation tasks to classification tasks, task incremental learning from basic tasks to complex tasks, and class incremental learning from few-class tasks to multiple-class tasks. The results of the experiment revealed that ECG-CL performed much better than training from scratch. Experiments reveal a potential for training a comprehensive ECG network for unobserved data and unique heart abnormalities. Experimentation with a single-lead dataset demonstrates the potential use of artificial intelligence algorithms to smart wearable devices for rather thorough daily monitoring. In the future, we want to create a knowledge backward transferrable model in order to better prior tasks. In addition, we want to construct a task-free continual learning network that will continually integrate information from newly-arrived data in order to enhance segmentation robust and complete classification categories.

REFERENCES

- [1] WHO, "Cardiovascular diseases (CVDs)," 2019. [Online]. Available: <https://www.who.int/en/newsroom/fact-sheets/detail/cardiovascular-diseases-cvds>
- [2] Z. Yang, Q. Zhou, L. Lei, K. Zheng, and W. Xiang, "An iot-cloud based wearable ecg monitoring system for smart healthcare," *Journal of Medical Systems*, vol. 40, no. 12, pp. 1–11, 2016.
- [3] H. Ozkan, O. Ozhan, Y. Karadana, M. Gulcu, S. Macit, and F. Husain, "A portable wearable tele-ecg monitoring system," *IEEE Transactions on Instrumentation and Measurement*, vol. 69, no. 1, pp. 173–182, 2019.
- [4] H. Gao, C. Liu, X. Wang, L. Zhao, Q. Shen, E. Ng, and J. Li, "An open-access ecg database for algorithm evaluation of qrs detection and heart rate estimation," *Journal of Medical Imaging and Health Informatics*, vol. 9, no. 9, pp. 1853–1858, 2019.
- [5] F. Liu, C. Liu, L. Zhao, X. Zhang, X. Wu, X. Xu, Y. Liu, C. Ma, S. Wei, Z. He, J. Li, and E. N. Y. Kwee, "An Open Access Database for Evaluating the Algorithms of Electrocardiogram Rhythm and Morphology Abnormality Detection," *Journal of Medical Imaging and Health Informatics*, vol. 8, no. 7, pp. 1368–1373, Sep. 2018.
- [6] P. Wagner, N. Strodthoff, R.-D. Bousseljot, W. Samek, and T. Schaeffter, "PTB-XL, a large publicly available electrocardiography dataset," 2020.
- [7] H. Gao, C. Liu, Q. Shen, and J. Li, *Representative Databases for Feature Engineering and Computational Intelligence in ECG Processing*. Singapore: Springer Singapore, 2020, pp. 13–29. [Online]. Available: https://doi.org/10.1007/978-981-15-3824-7_2
- [8] Z. Wang, W. Yan, and T. Oates, "Time series classification from scratch with deep neural networks: A strong baseline," in *2017 International Joint Conference on Neural Networks (IJCNN)*. IEEE, 2017, pp. 1578–1585.
- [9] J. Pan and W. J. Tompkins, "A real-time qrs detection algorithm," *IEEE Transactions on Biomedical Engineering*, no. 3, pp. 230–236, 1985.
- [10] W. Cai and D. Hu, "Qrs complex detection using novel deep learning neural networks," *IEEE Access*, vol. 8, pp. 97 082–97 089, 2020.
- [11] A. E. Johnson, J. Behar, F. Andreotti, G. D. Clifford, and J. Oster, "Multimodal heart beat detection using signal quality indices," *Physiological Measurement*, vol. 36, no. 8, p. 1665, 2015.
- [12] S. Kiranyaz, T. Ince, and M. Gabbouj, "Real-time patient-specific ecg classification by 1-d convolutional neural networks," *IEEE Transactions on Biomedical Engineering*, vol. 63, no. 3, pp. 664–675, 2015.
- [13] Z. Ebrahimi, M. Loni, M. Daneshmandi, and A. Gharehbaghi, "A review on deep learning methods for ecg arrhythmia classification," *Expert Systems with Applications: X*, vol. 7, p. 100033, 2020.
- [14] Z. Yu, J. Chen, Y. Liu, Y. Chen, T. Wang, R. Nowak, and Z. Lv, "Ddcnn: A deep learning model for af detection from a single-lead short ecg signal," *IEEE Journal of Biomedical and Health Informatics*, 2022.
- [15] S. Saadatnejad, M. Oveis, and M. Hashemi, "Lstm-based ecg classification for continuous monitoring on personal wearable devices," *IEEE Journal of Biomedical and Health Informatics*, vol. 24, no. 2, pp. 515–523, 2019.
- [16] S. S. Xu, M.-W. Mak, and C.-C. Cheung, "Towards end-to-end ecg classification with raw signal extraction and deep neural networks," *IEEE Journal of Biomedical and Health Informatics*, vol. 23, no. 4, pp. 1574–1584, 2018.
- [17] J. Xiao, J. Liu, H. Yang, Q. Liu, N. Wang, Z. Zhu, Y. Chen, Y. Long, L. Chang, L. Zhou *et al.*, "Ulegnet: An ultra-lightweight end-to-end ecg classification neural network," *IEEE Journal of Biomedical and Health Informatics*, vol. 26, no. 1, pp. 206–217, 2021.
- [18] Z. I. Attia, P. A. Noseworthy, F. Lopez-Jimenez, S. J. Asirvatham, A. J. Deshmukh, B. J. Gersh, R. E. Carter, X. Yao, A. A. Rabinstein, B. J. Erickson *et al.*, "An artificial intelligence-enabled ecg algorithm for the identification of patients with atrial fibrillation during sinus rhythm: a retrospective analysis of outcome prediction," *The Lancet*, vol. 394, no. 10201, pp. 861–867, 2019.
- [19] N. Sabor, G. Gendy, H. Mohammed, G. Wang, and Y. Lian, "Robust arrhythmia classification based on qrs detection and a compact 1d-cnn for wearable ecg devices," *IEEE Journal of Biomedical and Health Informatics*, 2022.
- [20] H. Zhao, J. Shi, X. Qi, X. Wang, and J. Jia, "Pyramid scene parsing network," in *Proceedings of the IEEE Conference on Computer Vision and Pattern Recognition (CVPR)*, 2017, pp. 2881–2890.
- [21] J. Wang, K. Sun, T. Cheng, B. Jiang, C. Deng, Y. Zhao, D. Liu, Y. Mu, M. Tan, X. Wang *et al.*, "Deep high-resolution representation learning for visual recognition," *IEEE Transactions on Pattern Analysis and Machine Intelligence*, vol. 43, no. 10, pp. 3349–3364, 2020.

- [22] L.-C. Chen, G. Papandreou, I. Kokkinos, K. Murphy, and A. L. Yuille, "DeepLab: Semantic image segmentation with deep convolutional nets, atrous convolution, and fully connected crfs," *IEEE Transactions on Pattern Analysis and Machine Intelligence*, vol. 40, no. 4, pp. 834–848, 2017.
- [23] T.-Y. Lin, P. Dollár, R. Girshick, K. He, B. Hariharan, and S. Belongie, "Feature pyramid networks for object detection," in *Proceedings of the IEEE Conference on Computer Vision and Pattern Recognition (CVPR)*, 2017, pp. 2117–2125.
- [24] O. Ronneberger, P. Fischer, and T. Brox, "U-net: Convolutional networks for biomedical image segmentation," in *International Conference on Medical Image Computing and Computer-assisted Intervention*. Springer, 2015, pp. 234–241.
- [25] P. Wagner, N. Strodthoff, R.-D. Bousselot, D. Kreiseler, F. I. Lunze, W. Samek, and T. Schaeffter, "PTB-XL, a large publicly available electrocardiography dataset," *Scientific Data*, vol. 7, no. 1, p. 154, 2020. [Online]. Available: <https://doi.org/10.1038/s41597-020-0495-6>
- [26] A. Peimankar and S. Puthusserypady, "Dens-ecg: A deep learning approach for ecg signal delineation," *Expert Systems with Applications*, vol. 165, p. 113911, 2021.
- [27] X. Liu, H. Wang, Z. Li, and L. Qin, "Deep learning in ecg diagnosis: A review," *Knowledge-Based Systems*, vol. 227, p. 107187, 2021.
- [28] X. Xie, H. Liu, D. Chen, M. Shu, and Y. Wang, "Multilabel 12-lead ecg classification based on leadwise grouping multibranch network," *IEEE Transactions on Instrumentation and Measurement*, vol. 71, pp. 1–11, 2022.
- [29] J. Zhang, A. Liu, M. Gao, X. Chen, X. Zhang, and X. Chen, "Ecg-based multi-class arrhythmia detection using spatio-temporal attention-based convolutional recurrent neural network," *Artificial Intelligence in Medicine*, vol. 106, p. 101856, 2020.
- [30] N. Strodthoff, P. Wagner, T. Schaeffter, and W. Samek, "Deep learning for ECG analysis: Benchmarks and insights from PTB-XL," *IEEE Journal of Biomedical and Health Informatics*, vol. 25, no. 5, pp. 1519–1528, 2021. [Online]. Available: <https://doi.org/10.1109/jbhi.2020.3022989>
- [31] E. A. P. Alday, A. Gu, A. J. Shah, C. Robichaux, A.-K. I. Wong, C. Liu, F. Liu, A. B. Rad, A. Elola, S. Seyedi *et al.*, "Classification of 12-lead ecgs: the physionet/computing in cardiology challenge 2020," *Physiological Measurement*, vol. 41, no. 12, p. 124003, 2020.
- [32] M. Salem, S. Taheri, and J. Yuan, "Ecg arrhythmia classification using transfer learning from 2- dimensional deep cnn features," in *2018 IEEE Biomedical Circuits and Systems Conference (BioCAS)*, 2018, pp. 1–4.
- [33] K. Weimann and T. O. Conrad, "Transfer learning for ecg classification," *Scientific Reports*, vol. 11, no. 1, pp. 1–12, 2021.
- [34] A. Raza, K. P. Tran, L. Koehl, and S. Li, "Designing ecg monitoring healthcare system with federated transfer learning and explainable ai," *Knowledge-Based Systems*, vol. 236, p. 107763, 2022.
- [35] D. Kiyasseh, T. Zhu, and D. Clifton, "A clinical deep learning framework for continually learning from cardiac signals across diseases, time, modalities, and institutions," *Nature Communications*, vol. 12, no. 1, pp. 1–11, 2021.
- [36] R. He, Y. Liu, K. Wang, N. Zhao, Y. Yuan, Q. Li, and H. Zhang, "Automatic detection of qrs complexes using dual channels based on u-net and bidirectional long short-term memory," *IEEE Journal of Biomedical and Health Informatics*, vol. 25, no. 4, pp. 1052–1061, 2020.
- [37] M. Gabbouj, S. Kiranyaz, J. Malik, M. U. Zahid, T. Ince, M. E. Chowdhury, A. Khandakar, and A. Tahir, "Robust peak detection for holter ecgs by self-organized operational neural networks," *IEEE Transactions on Neural Networks and Learning Systems*, 2022.
- [38] A. Y. Hannun, P. Rajpurkar, M. Haghpasahi, G. H. Tison, C. Bourn, M. P. Turakhia, and A. Y. Ng, "Cardiologist-level arrhythmia detection and classification in ambulatory electrocardiograms using a deep neural network," *Nature Medicine*, vol. 25, no. 1, pp. 65–69, 2019.
- [39] G. H. Tison, J. Zhang, F. N. Dellling, and R. C. Deo, "Automated and interpretable patient ecg profiles for disease detection, tracking, and discovery," *Circulation: Cardiovascular Quality and Outcomes*, vol. 12, no. 9, p. e005289, 2019.
- [40] Y. Zhang, J. Li, S. Wei, F. Zhou, and D. Li, "Heartbeats classification using hybrid time-frequency analysis and transfer learning based on resnet," *IEEE Journal of Biomedical and Health Informatics*, vol. 25, no. 11, pp. 4175–4184, 2021.
- [41] G. M. van de Ven and A. S. Tolias, "Three scenarios for continual learning," *arXiv: Learning*, 2019.
- [42] H. Qu, H. Rahmani, L. Xu, B. Williams, and J. Liu, "Recent advances of continual learning in computer vision: An overview," *arXiv preprint arXiv:2109.11369*, 2021.
- [43] J. Kirkpatrick, R. Pascanu, N. Rabinowitz, J. Veness, G. Desjardins, A. A. Rusu, K. Milan, J. Quan, T. Ramalho, A. Grabska-Barwinska *et al.*, "Overcoming catastrophic forgetting in neural networks," *Proceedings of the National Academy of Sciences*, vol. 114, no. 13, pp. 3521–3526, 2017.
- [44] F. Zenke, B. Poole, and S. Ganguli, "Continual learning through synaptic intelligence," *Proceedings of the International Conference on Machine Learning (ICML)*, 2017.
- [45] X. He and H. Jaeger, "Overcoming catastrophic interference using conceptor-aided backpropagation," *Learning*, 2018.
- [46] S. Ebrahimi, M. Elhoseiny, T. Darrell, and M. Rohrbach, "Uncertainty-guided continual learning with bayesian neural networks," *Proceedings of the International Conference on Learning Representations (ICLR)*, 2020.
- [47] A. Chaudhry, M. Rohrbach, M. Elhoseiny, T. Ajanthan, P. K. Dokania, P. H. S. Torr, and M. Ranzato, "On tiny episodic memories in continual learning," *arXiv: Learning*, 2019.
- [48] C. V. Nguyen, Y. Li, T. D. Bui, and R. E. Turner, "Variational continual learning," *Proceedings of the International Conference on Learning Representations (ICLR)*, 2017.
- [49] D. Lopez-Paz and M. Ranzato, "Gradient episodic memory for continual learning," *Proceedings of the Neural Information Processing Systems (NeurIPS)*, 2017.
- [50] C. Fernando, D. Banarse, C. Blundell, Y. Zwols, D. Ha, A. Rusu, A. Pritzel, and D. Wierstra, "Pathnet: Evolution channels gradient descent in super neural networks," *arXiv: Neural and Evolutionary Computing*, 2017.
- [51] J. Yoon, E. Yang, J. Lee, and S. J. Hwang, "Lifelong learning with dynamically expandable networks," *Learning*, 2017.
- [52] A. Mallya and S. Lazebnik, "Packnet: Adding multiple tasks to a single network by iterative pruning," *Proceedings of the IEEE Conference on Computer Vision and Pattern Recognition (CVPR)*, 2017.
- [53] J. Hu, L. Shen, and G. Sun, "Squeeze-and-excitation networks," in *Proceedings of the IEEE Conference on Computer Vision and Pattern Recognition (CVPR)*, 2018, pp. 7132–7141.
- [54] ISO Central Secretary, "Health informatics – standard communication protocol – part 91064: Computer-assisted electrocardiography," International Organization for Standardization, Geneva, CH, Standard ISO 11073-91064:2009, 2009. [Online]. Available: <https://www.iso.org/standard/91064.html>